

RESTRICTED

26223  
CoA. Note No. 156  
MAY

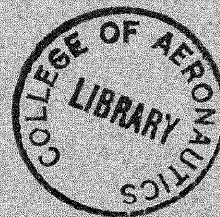


THE COLLEGE OF AERONAUTICS  
CRANFIELD

A MEASUREMENT OF THE RADIATED NOISE ON A  
SUBSONIC JET AIRCRAFT IN GLIDING FLIGHT

by

D. HYDE



Prepared under Ministry of Aviation Contract No. KD/18/07/C. B. 6(c).

RESTRICTED

26223  
B

3 8006 10057 8767

- RESTRICTED -

NOTE NO. 156

JUNE, 1963

THE COLLEGE OF AERONAUTICS

CRANFIELD

A Measurement of the Radiated Noise on a Subsonic Jet

Aircraft in Gliding Flight

- by -

D. Hyde, M.Sc.(Eng), D.I.C., A.C.G.I.

SUMMARY

The noise radiated from a gliding subsonic jet aircraft was measured in flight by a probe microphone installed in a 'laminarised' boom projecting from the fin of the aircraft. As the signal associated with the windmilling turbines was predominant even at flight speeds near the aircraft's limiting Mach number, it was not possible to relate the noise radiated from the turbulent boundary layers to flight speed.

The measured sound pressure levels in the frequency band 40 c/s to 15 kc/s, for Mach numbers between 0.24 and 0.66 at an altitude of 20,000 ft., were in the range from 110 to 115 decibels relative to 0.0002  $\mu$ bar. A calculation of the radiated noise from the boundary layers gave overall levels of 85 to 120 db relative to 0.0002  $\mu$ bar at the microphone position on the aircraft for the same range of flight conditions.



Prepared under Ministry of Aviation Contract No. KD/18/07/C.B.6(c).

- RESTRICTED -

Contents

	<u>Page</u>
Summary	
List of symbols	
1. Introduction	1
2. Experimental equipment and technique	1
2.1 Aircraft	1
2.2 Instrumentation	1
2.3 Flight technique	2
3. Tests performed	2
4. Results	3
4.1 Analysis	3
4.2 Errors	3
5. Discussion	3
5.1 Experimental results	3
5.2 Calculation of boundary layer noise	5
6. Conclusions	7
7. Future work	7
8. Acknowledgements	8
9. References	8

List of tables

1(a) Sound pressure levels - Ground runs	9
1(b) Sound pressure levels - Flight 1	9
1(c) Sound pressure levels - Flight 2	10
1(d) Sound pressure levels - Flight 3	10

List of Figures

1. The probe microphone installation
2. The M.S.760 'Paris' aircraft (microphone boom fitted)
3. Free field calibration of probe microphone
4. Overall frequency response of tape equipment
5. SPL from radiated noise as a function of Mach number

6. SPL in turbulent boundary layer as a function of Mach number
  - 7(a) Spectra (corrected) - Ground runs
  - 7(b) Spectra (corrected) - Transition ring off
  - 7(c) Spectra (corrected) - Transition ring on
8. Calculated overall SPL at microphone position as a function of Mach number

- RESTRICTED -

List of symbols

$C_L$	aircraft lift coefficient
$\alpha$	incidence of wing mean chord relative to freestream
SPL	sound pressure level in decibels relative to 0.0002 $\mu$ bar
q	dynamic pressure
$\sqrt{\overline{p^2}}$	root mean square pressure fluctuations
$c_f$	skin friction coefficient
d	diameter of microphone sensing hole
$\delta^*$	boundary layer displacement thickness
$\omega$	circular frequency
$U_o$	freestream velocity

## 1. Introduction

Recent work by Pfenninger<sup>1</sup> of the Norair Group of Northrop Corporation has emphasized the importance of the radiated turbulent boundary layer noise associated with the unsucked areas of a laminar flow vehicle. Together with the sound generated by the propulsion system, this source of noise may be sufficient to cause transition on such a low drag suction aircraft.

The object of these tests was to establish the order of magnitude, and the dependence on aircraft forward speed, of the noise radiated from the turbulent boundary layers on a subsonic jet aircraft. After this work began, the writer obtained a Norair report<sup>2</sup> which included some comparable measurements on a B-66 aircraft, and also empirical formulae for estimating the overall level of this source of noise.

## 2. Experimental equipment and technique

### 2.1. Aircraft

The aircraft used was a Morane Saulnier M.S.760 Paris I, powered by two Turbomeca Marbore engines. Limitations on equivalent airspeed and Mach number were 350 knots and 0.7 respectively.

Wing area was 198 sq.ft. and the inboard section was NACA 64A 113.5, changing to NACA 64A112 at the mid semi-span station. Although it was probable that the flow over the wing was turbulent under all flight conditions, roughness strips were attached to the upper surface, near the leading edge, in order to guarantee this condition.

The microphone was mounted in a 1 inch diameter boom (Figure 1) which projected 42 inches from near the top of the aircraft's fin, this being the only suitable position which placed the boom in the far field relative to the wing boundary layer noise (Figure 2). Previous work<sup>3</sup> using this same boom in the wind tunnel and in flight indicated that laminar flow could be expected at the microphone sensing hole for speeds up to the limiting condition on the aircraft and for an incidence range of  $-1^{\circ}$  to  $+2^{\circ}$ . As the incidence range of the aircraft corresponding to its speed range was approximately  $9^{\circ}$ , provision was made to mount the microphone boom at several incidences relative to the aircraft datum.

### 2.2. Instrumentation

A Brüel and Kjaer Type 4133 half-inch diameter condenser microphone, with the associated Type 2615 cathode follower, was used. The transducer was employed as a probe microphone by connecting the microphone cartridge to a 4 mm flush static hole on the elliptic nosed boom by means of a 4 mm coupling tube (Figure 1). By mounting the whole unit in polyurethane foam, spurious signals arising from the mechanical

vibration of the boom were minimised.

The acoustical resonances in the probe tube were damped by a polyurethane foam plug. A foam plug was found to be equally effective and less likely to shift when vibrated than the steel wool material recommended by Brüel and Kjaer. The flattest frequency response of the probe tube was obtained by adjusting the size of the plug. Coarse adjustment was achieved using the Brüel and Kjaer calibration coupler from the Type UA 0040 Probe Microphone Kit. Finally, a free field frequency response was obtained for the microphone-boom installation using an unmodified half-inch microphone as a standard and a loud speaker by a white noise signal as a sound source. This free field characteristic was measured before and after each flight to ensure that it had not changed (typical curves for a flight are shown in Figure 3).

The directional properties of this free field characteristic were also investigated using the same sound source. Although the speaker itself was not highly directional, it could be seen that there was no large effect due to incident sound within the range of  $\pm 90^\circ$  in planes along, and perpendicular to, the boom axis, except in the limiting case of grazing incidence.

The microphone output was recorded using a Flexonics A4011 tape recorder using the direct recording process at a tape speed of 15 ins./sec. In the range from 40 c/s to 15 kc/s the corresponding overall record/replay frequency response was within  $\pm 2$  db (Figure 4). A stepped attenuator and monitoring instrument were located between the transducer and the tape deck so that the recorded signal was always of reasonable magnitude relative to the tape saturation level. For the analysis of the recorded tapes a Flexonics 409 ground replay machine was used.

### 2.3. Flight technique

Recordings were taken as the aircraft passed through an altitude of 20,000 ft. with both engines throttled back; some runs were repeated with the starboard turbine completely shut down. This procedure was used in an attempt to minimise the engine noise.

### 3. Tests performed

With the microphone boom at an incidence of  $0^\circ$  relative to the aircraft datum, a series of readings were taken. For comparative purposes, a transition ring was then fixed on the boom 4 inches ahead of the microphone sensing hole, and a second flight completed.

Finally the boom was set at  $-4^\circ$  relative to the aircraft datum and a third set of recordings obtained.

Ground records were also taken, with one turbine at two typical

windmill R.P.M., both with the microphone boom rigidly installed and with the boom hand held in the same position (Table 1).

#### 4. Results

##### 4.1 Analysis

A one-third octave analysis was carried out on the flight tapes, using a Brüel and Kjaer Type 2107 frequency analyser, over the frequency range of 40 c/s to 15 kc/s.

These one-third octave readings were corrected for the free field characteristic of the probe microphone and the frequency response of the tape equipment in order to calculate the sound pressure levels. Account was also taken of the polarisation voltage across the transducer (if different from the nominal 200 volts) and the change in sensitivity due to altitude. Finally the sound pressure levels per cycle of bandwidth were found and the resulting spectra plotted (Figure 7).

##### 4.2 Errors

The absolute calibration of the microphone was checked by a Brüel and Kjaer Type 4220 Pistonphone to an accuracy of  $\pm 0.2$  db. No temperature compensation has been applied to the results as this is not specified precisely for the transducer, but it is less than  $\pm 0.3$  db for the temperature range involved.

The overall accuracy of the results is probably within  $\pm 1.5$  db, although the repeatability on a given flight is much better than this.

As a ground check on the system accuracy, a source of white noise was recorded simultaneously via the microphone boom/tape recorder set-up in the aircraft, and by a standard transducer in a similar position coupled directly to an overall level meter. After the appropriate frequency analysis and correction process, the two overall sound pressure levels were within 10% of each other.

#### 5. Discussion

##### 5.1 Experimental results

Table 1 summarises the overall level measurements taken, together with the appropriate test conditions.

From the ground runs (Table 1(a)), it can be seen that the levels corresponding to the rigidly attached and hand held boom cases were well within the overall system accuracy. This was a good indication that spurious output signals due to the vibration of the boom were not significant, especially as the boom vibration would probably be less severe in flight than on the ground. This result was expected as the microphone had been flexibly supported in polyurethane foam, and also



because the natural frequency of the boom (16 c.p.s.) was below the cut-off frequency of the tape equipment.

Figure 6(a) illustrates the spectra of two ground runs with one turbine operating at 15,000 and 16,000 R.P.M. i.e. typical windmill R.P.M. under test conditions. Remembering that a one-third octave analysis was used, peaks may be identified that correspond to the turbine shaft frequency and its first harmonic (250/500 c.p.s. and 267/533 c.p.s. respectively). The peaks at 3,800 c.p.s. and 7,700 c.p.s. are associated with the product of shaft frequency and the number of turbine blades; however, as there are 37 blades on the rotor and 25 on the stator, beat effects will occur and the peaks correspond to the product of the shaft frequency and a figure that is greater than 25 but less than 37.

For the first flight the boom was set at 0° incidence relative to the aircraft datum. Assuming that the local flow direction at the boom was the same as in the freestream, and a boom incidence tolerance of -1° to +2°, then the  $C_L$ - $\alpha$  relationship for the aircraft indicated that laminar flow would prevail over the microphone hole for a range of true airspeeds from 390 to 680 ft./sec. at 20,000 ft. altitude for typical aircraft test weights.

The measured SPLs are between 109.7 db and 115.2 db. Figure 5 shows that the SPL-true airspeed relationship is essentially constant over the major part of the speed range, showing a tendency to increase appreciably only above a T.A.S. of 600 ft./sec. At T.A.S.s below 350 ft./sec. the small increase in SPL may be attributed to the transition of the boundary layer over the microphone static hole to the turbulent state. In Figure 7(b) spectra are plotted for three of the flight conditions.

The second flight was made with the boom incidence again at 0°, but with a transition wire placed 4 ins. ahead of the microphone sensing position. Table 1(c) shows the SPLs recorded and Figure 6 presents these results graphically; the spectra at three flight speeds are plotted in Figure 7(c). From the results of Willmarth<sup>4</sup> and others, it would be expected that the R.M.S. pressure fluctuations would be proportional to the square of speed; as on the first flight, it can be seen that this only becomes true in the high speed range.

Willmarth has also shown that in a turbulent boundary layer the root mean square pressure fluctuations  $\sqrt{\overline{p}^2} \propto q \cdot c_f$  and, assuming a value of 0.003 for  $c_f$ ,  $\sqrt{\overline{p}^2} \approx 0.006q$ . The reasons for the difference in magnitude between the 0.006q law and the experimental SPLs measured on Flight 2 at the higher speeds are:

- (1) the finite value of the ratio of the diameter of the microphone sensing hole to the boundary layer displacement thickness. Using 'flat plate' formulae as a first approximation, it can be shown

that  $d/\delta^* \approx 12$  in the present tests in the high speed range. Hodgson<sup>5</sup> has shown that the measured value of  $\sqrt{(p)}$  will be reduced by a factor of 4 for a value of  $d/\delta^* = 12$ .

- (2) the cut-off frequency of the measuring apparatus. From the collected data of various experimental workers<sup>6,7</sup> it can be seen that the turbulent boundary layer spectrum is fairly flat at frequencies up to values for  $\frac{\omega \delta^*}{U_0}$  of at least 0.4, and then falls off with increasing frequency at frequencies above this. At  $U_0 = 700$  ft./sec. the corresponding frequency is 53 kc/s, whereas the effective cut-off frequency of the tape gear was 15 kc/s. It must also be remembered that the high frequency section, where the spectrum is falling off, still contributes an appreciable proportion of the total energy.

At the lower speeds in Flight 2 the magnitude of the experimental SPLs approached, or even exceeded, the values appropriate to the 0.006q law (Figure 6) due to a combination of three effects. Firstly, the relative magnitude of the radiated noise from the aircraft's turbines becomes more important at lower speeds; secondly, the values of the ratio  $d/\delta^*$  become smaller (at  $U_0 = 250$  ft./sec.,  $d/\delta^* \approx 8$ ); and thirdly, the frequency appropriate to a value of  $\frac{\omega \delta^*}{U_0} = 0.4$  becomes less as speed is decreased (at  $U_0 = 250$  ft./sec., the corresponding frequency is 13 kc/s).

For the third flight the boom was reset at  $-4^\circ$  incidence relative to the aircraft datum in order to confirm that the measurements were not very dependent on boom incidence. Table 1(d) and Figure 5 show that the SPLs were again essentially constant over a T.A.S. range of 250-535 ft./sec., the magnitudes being between 112 and 114 db. Considering the overall system accuracy, these last results were essentially of the same magnitude as the first flight data.

## 5.2 Calculation of boundary layer noise

The method detailed in Reference 2 was used to compute the radiated turbulent boundary layer noise; for convenience this technique is outlined in this sub-section.

As the most probable explanation of the noise radiated from turbulent boundary layers is the quadrupole theory of Lighthill, similarities should exist between the characteristics of jet noise and those of boundary layer noise. The total acoustic power radiation from the boundary layer may be calculated knowing the appropriate effective noise radiating area of the equivalent jet, and assuming that the noise power generated per unit surface area in the boundary layer is constant and independent of the distance from the transition point.

To predict the noise radiated to a point on a moving aircraft, the following three factors must also be considered:

- (1) the spacial distribution of the acoustic power relative to the radiating surface.
- (2) the effect of aircraft motion on the propogation of noise from the radiating surface to the receiving point.
- (3) the summation of noise radiated from many surfaces distributed over the aircraft.

For a flat plate of surface area  $\Delta S$ , distance R from receiving point,

$$\Delta SPL = \left[ 139 + 10 \log \frac{\rho_{\infty}^2 a_{\infty}^4}{\rho_0^2 a_0^4} + 10 \log M_{\infty}^8 + 10 \log \frac{\Delta S}{R^2} + 10 \log f(\phi) + \log g(M) \right] \text{ db} \quad (1)$$

where  $\rho_{\infty}$   $a_{\infty}$   $M_{\infty}$  are freestream density, speed of sound and Mach number

$\rho_0$   $a_0$  are standard sealevel density and speed of sound

$f(\phi)$  is the directivity function

$g(M)$  is the motion correction function

For a cylinder of body diameter D, radial distance R from receiving point,

$$\Delta SPL = \left[ 134 + 10 \log \frac{\rho_{\infty}^2 a_{\infty}^4}{\rho_0^2 a_0^4} + 10 \log M_{\infty}^8 + \log \frac{D}{R} + 10 \log F \right] \text{ db} \quad (2)$$

where F is a function of the geometrical relationship of the receiving point with the body and is dependent on Mach number.

The mean square pressure fluctuations at the microphone position on the Paris aircraft were computed for the following five parts of the aircraft, and them summed to find the total mean square value:

- (1) the wing was divided into 6 subareas and equation (1) used.
- (2) the fuselage, because of its flattened cylindrical shape, was considered as two sections using both equations (1) and (2) and the mean result found. The nose section forward of the canopy was ignored as it was effectively shielded from the microphone

position and the contribution from the fuselage section above the tail skid was included in part (4).

- (3) the tailplane was divided into 2 subareas and equation (1) used.
- (4) the fin and rudder using equation (1).
- (5) the tip tanks, using equation (2).

The contributions and total SPL at the microphone position are plotted as a function of Mach number in Figure 8. The total calculated SPL is also superimposed on the experimental results in Figure 5, from which it can be seen that the radiated boundary layer noise only becomes appreciable, compared with the noise from the windmilling turbines, above a true airspeed of 500 ft./sec. It appears from Figure 5 that the calculation method tends to overestimate the radiated noise, although the evidence is extremely restricted. However, as is emphasised in Reference 5, absolute agreement on magnitude would indeed be surprising considering all the assumptions involved, particularly recognizing that the velocity profiles in the turbulent boundary layer are not identically similar to those in a free jet.

## 6. Conclusions

The noise radiated from the aircraft's windmilling turbines was predominant over the Mach number range of 0.24 to 0.66 at an altitude of 20,000 ft. SPLs in the range from 110 to 115 db for the frequency band 40 c/s to 15 kc/s were measured at a position in front of the fin under these flight conditions.

Norair's calculation method for the prediction of radiated turbulent boundary layer noise alone gave a range of SPLs of 85 to 120 db for the same flight regime. Although the experimental evidence is severely limited, it appears that this calculation method gives the correct order of magnitude for radiated boundary layer noise, but may overestimate the overall level.

## 7. Future work

As the major noise generating mechanism from the turbulent boundary layer is of a quadrupole nature, the importance of this source increases rapidly as flight speed is increased. An in-flight measurement of radiated noise which included supersonic conditions would provide further useful confirmation of the Norair subsonic estimation formulae, together with an invaluable extension to the supersonic regime.

It is recommended that a contract for such work should be negotiated and it is suggested that an English Electric Lightning aircraft would be a suitable test vehicle that could be made available.

## 8. Acknowledgements

The author wishes to thank Professor G.M. Lilley, Department of Aerodynamics, for his suggestions and interest in this work and Mr. M.A. Perry, Department of Flight, for arranging the aircraft instrumentation and analysis equipment.

## 9. References

1. Pfenninger, W. and Bacon, J.W. Influence of acoustical disturbances on the behaviour of a swept laminar suction wing.  
Norair Division of Northrop Corporation Report NB 62 - 105, Section I, Part 3. Revised, August 1962.
2. Rooney, R. Carmichael, R.F. and Eldred, K.M. Investigation of noise with respect to the LFC, NB-66 aircraft.  
Norair Division of Northrop Corporation Report NOR-61-10. April, 1961.
3. Trayford, R.S. External noise level on Lancaster PA 474.  
College of Aeronautics Note No. 138. February, 1963.
4. Wilmarth, W.W. Wall pressure fluctuations in a turbulent boundary layer.  
NACA TN 4139. March, 1958.
5. Hodgson, T.H. Pressure fluctuations in shear flow turbulence.  
College of Aeronautics Note No. 129. May, 1962.
6. Richards, E.J. Bull, M.K. and Willis, J.L. Boundary layer noise research in U.S.A. and Canada.  
U.S.A.A. Report No. 131. February, 1960.
7. Bull, M.K. and Willis, J.L. Some results of experimental investigations of the surface pressure field due to a turbulent boundary layer.  
A.A.S.U. Report No. 199. November, 1961.

TABLE 1(a)

SOUND PRESSURE LEVELS - GROUND RUNS

PORT TURBINE RPM	MICROPHONE BOOM	SPL	
		$\mu$ BAR	DB RE .0002 $\mu$ BAR
16,000	} RIGIDLY	{ 150	117.5
15,000			
16,000	} HAND-HELD	{ 168	118.5
15,000			

TABLE 1(b)

SOUND PRESSURE LEVELS - FLIGHT 1

RUN NO.	TRUE AIRSPEED FT/SEC.	STBD TURBINE SHUT DOWN	WINDMILL RPM		SPL	
			PORT	STBD	$\mu$ BAR	DB RE .0002 $\mu$ BAR
1	249	NO	15,000	8,500	71	111.0
2	274	NO	15,000	9,000	67	110.5
3	319	NO	15,000	12,000	69	110.8
4	364	NO	15,500	12,000	61	109.7
5	450	NO	15,500	13,500	74	111.4
6	535	NO	16,000	15,000	83	112.4
7	678	NO	16,000	15,000	115	115.2
8	535	YES	15,000	2,000	81	112.1
9	249	YES	15,000	3,000	79	111.9

TABLE 1(c)  
SOUND PRESSURE LEVELS - FLIGHT 2

RUN NO.	TRUE AIRSPEED FT./SEC.	STBD TURBINE SHUT DOWN	WINDMILL RPM		SPL	
			PORT	STBD	μBAR	DB RE .0002 μBAR
1	249	NO	15,500	10,500	115	115.2
2	317	NO	15,700	13,200	127	116.1
3	450	NO	16,200	14,300	158	118.0
4	533	NO	16,200	15,400	165	118.3
5	683	NO	16,000	15,000	235	121.4
6	366	NO	16,000	13,900	127	116.1
7	276	NO	15,200	12,900	111	114.9
8	722	NO	16,400	16,000	310	123.8
9	600	NO	16,500	16,000	203	120.1
10	538	YES	16,400	4,100	170	118.6
11	251	YES	15,000	2,000	102	114.1
12	722	YES	16,500	6,000	277	122.8
13	366	YES	15,750	2,000	134	116.5
14	600	YES	16,000	5,000	196	119.8
15	452	YES	15,600	2,500	141	117.0

TABLE 1(d)  
SOUND PRESSURE LEVELS - FLIGHT 3

RUN NO.	TRUE AIRSPEED FT./SEC.	STBD TURBINE SHUT DOWN	WINDMILL RPM		SPL	
			PORT	STBD	μBAR	DB RE .0002 μBAR
1	251	NO	15,000	8,500	85	112.6
2	272	NO	15,000	8,250	80	112.0
3	364	NO	15,500	13,250	91	113.2
4	450	NO	15,500	13,000	93	113.4
5	535	NO	16,000	15,000	101	114.1
6	249	YES	14,500	1,000	83	112.4

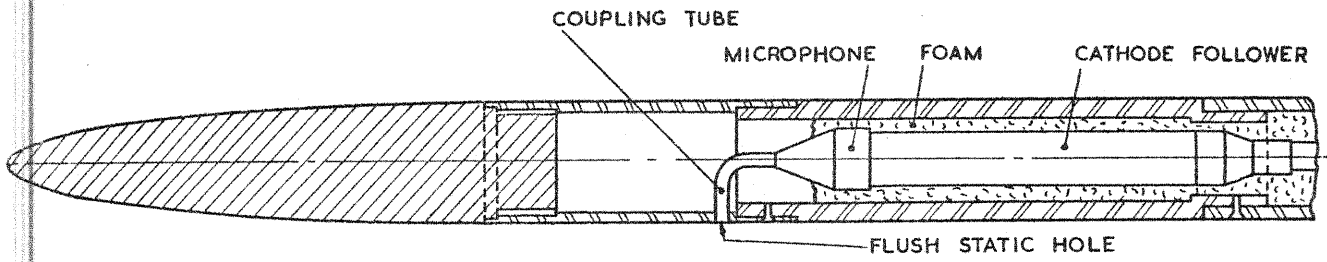


FIG. 1. THE PROBE MICROPHONE INSTALLATION.

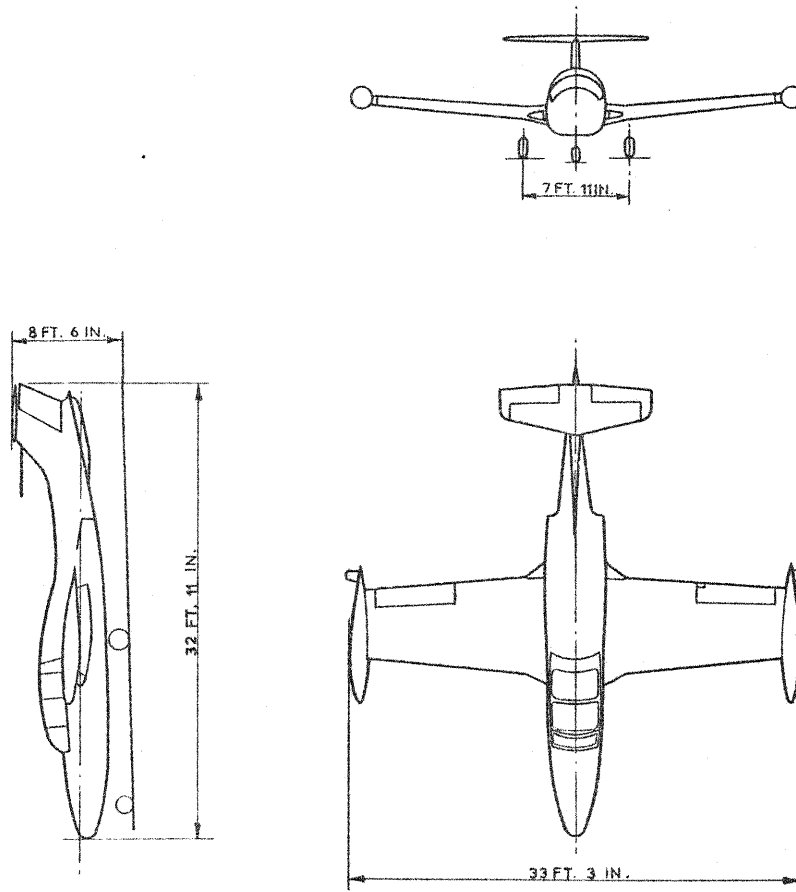
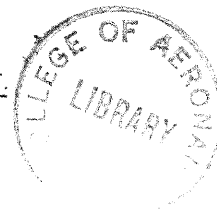


FIG. 2. THE M.S.760 'PARIS' AIRCRAFT.  
(MICROPHONE BOOM FITTED)





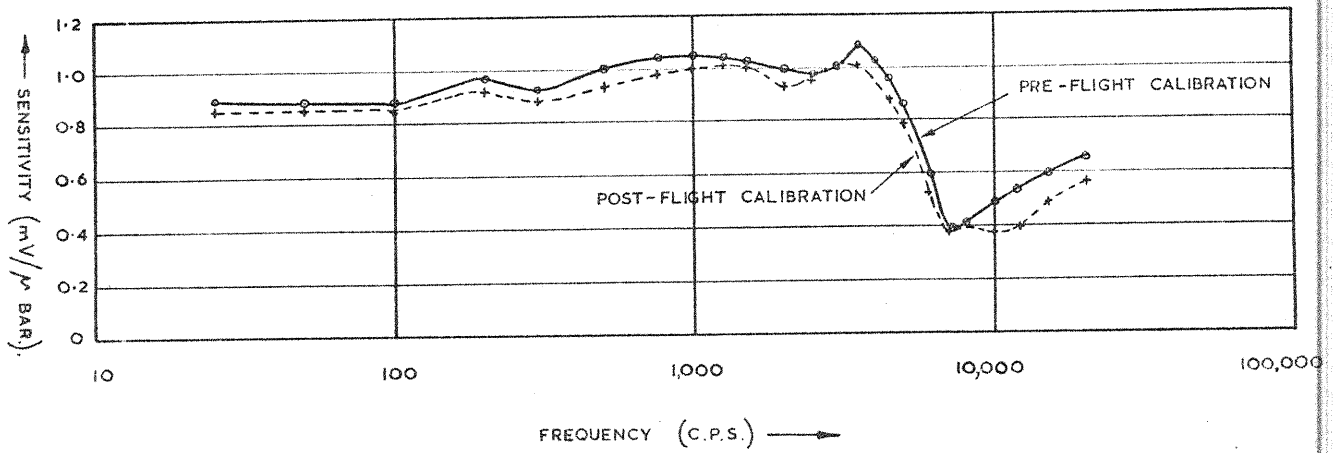


FIG. 3. FREE FIELD CALIBRATION OF PROBE MICROPHONE.

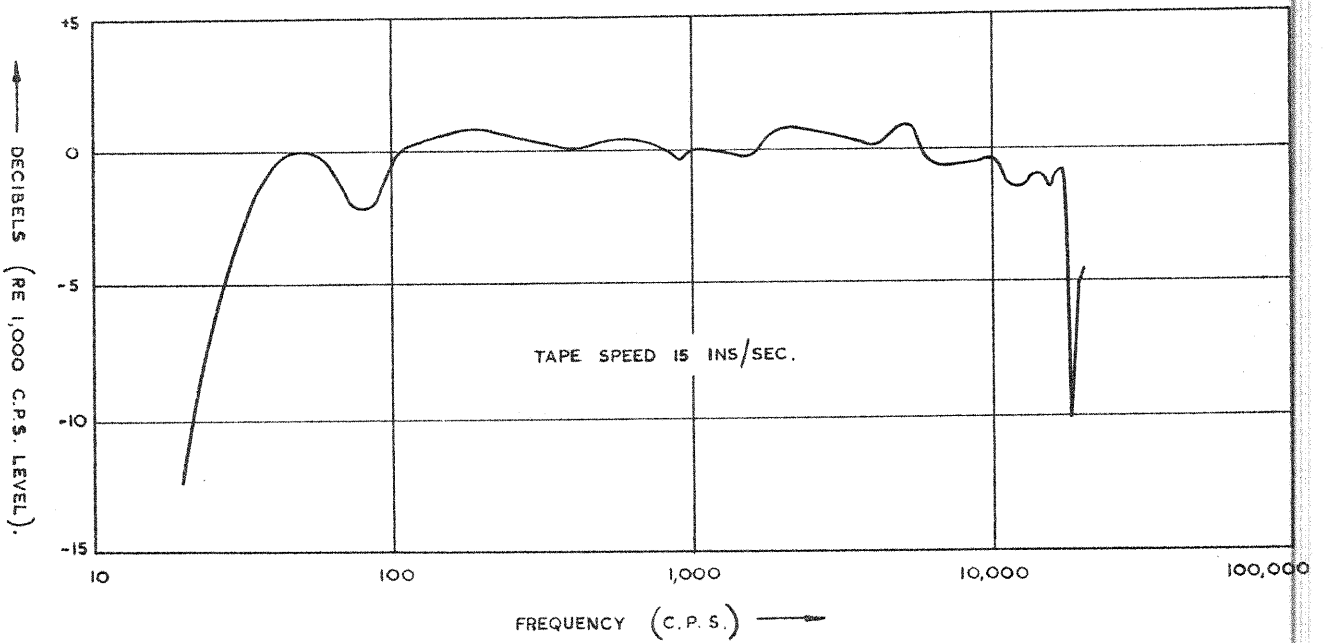


FIG. 4. OVERALL FREQUENCY RESPONSE OF TAPE EQUIPMENT.

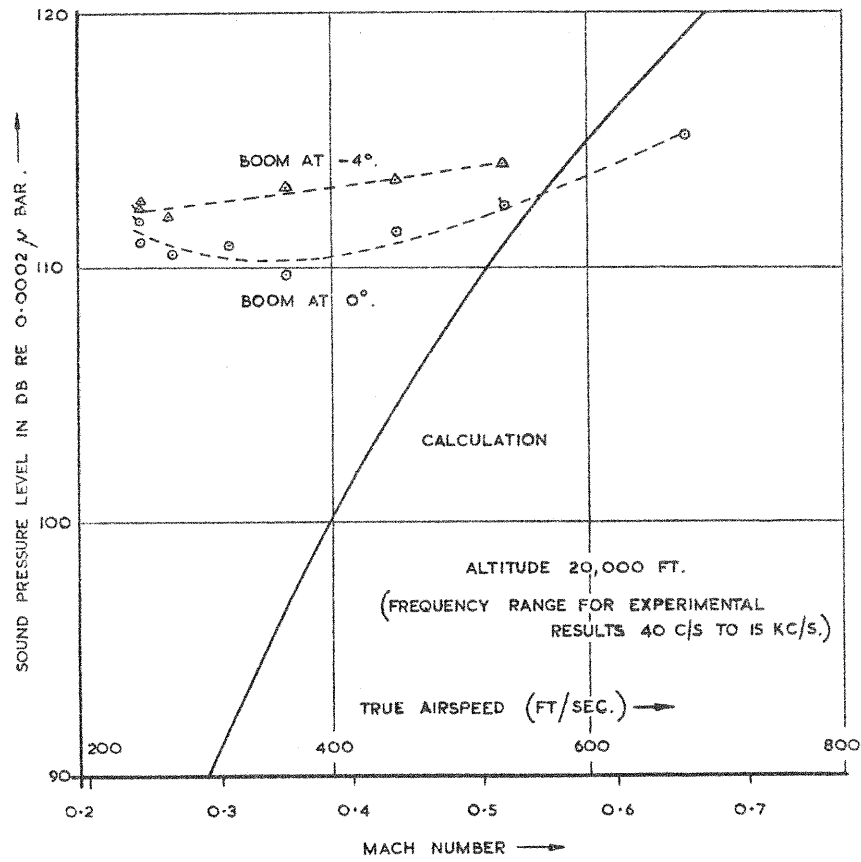


FIG. 5. SPL FROM RADIATED NOISE AS A FUNCTION OF MACH NUMBER.

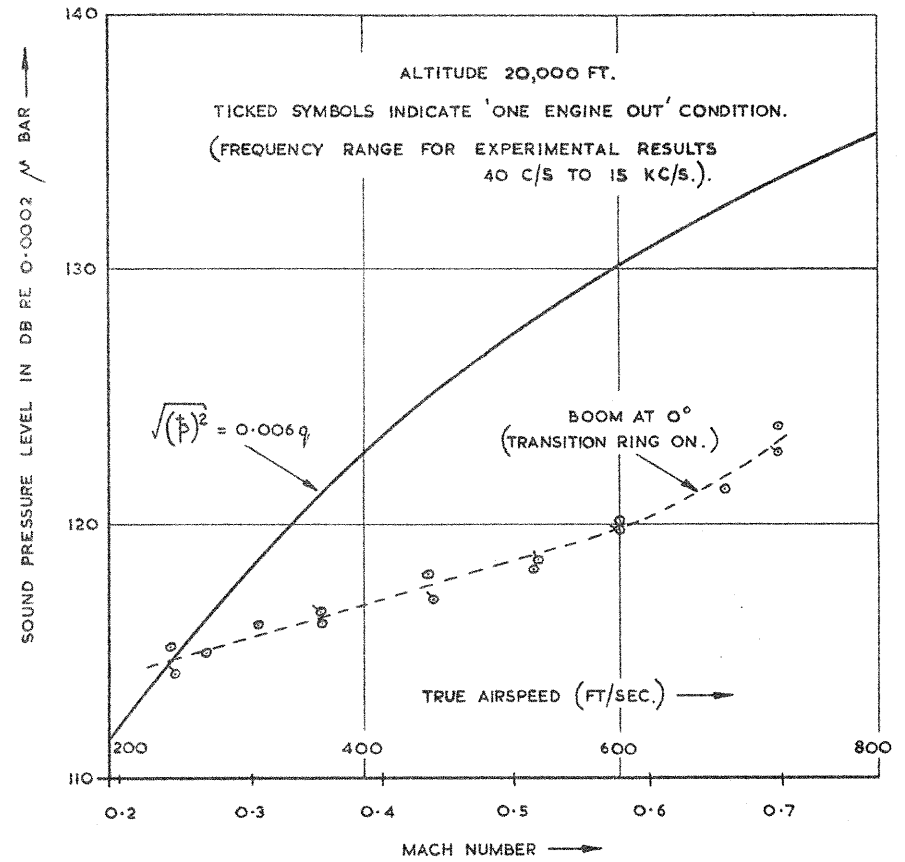


FIG. 6. SPL IN TURBULENT BOUNDARY LAYER AS A FUNCTION OF MACH NUMBER.

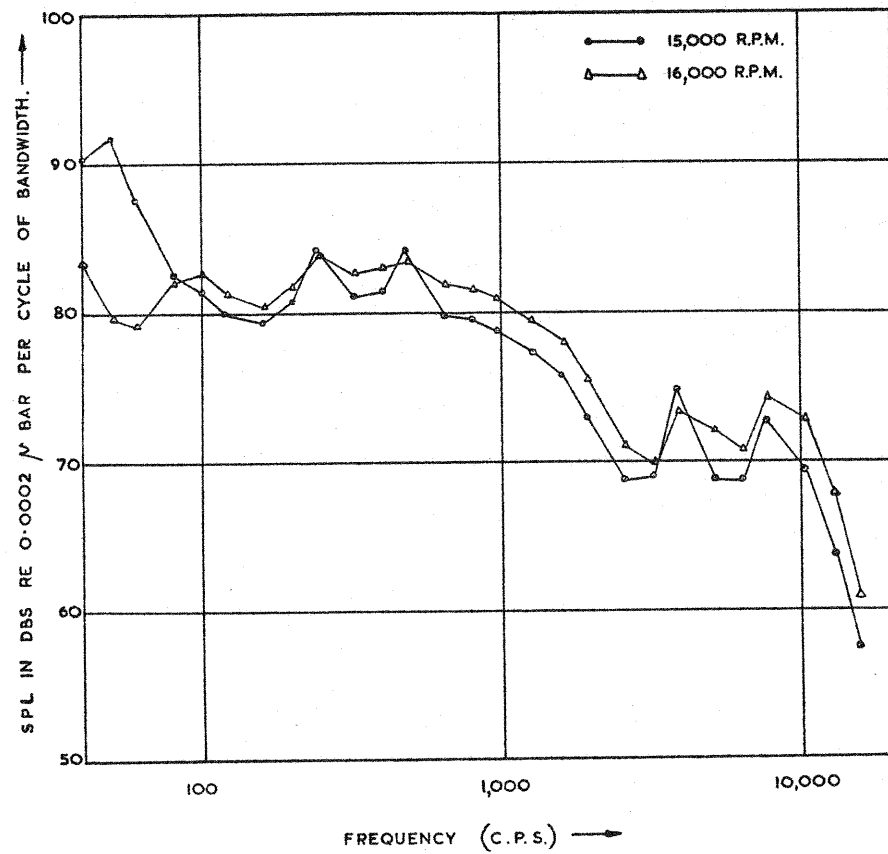


FIG. 7(a). SPECTRA (CORRECTED) - GROUND RUNS.

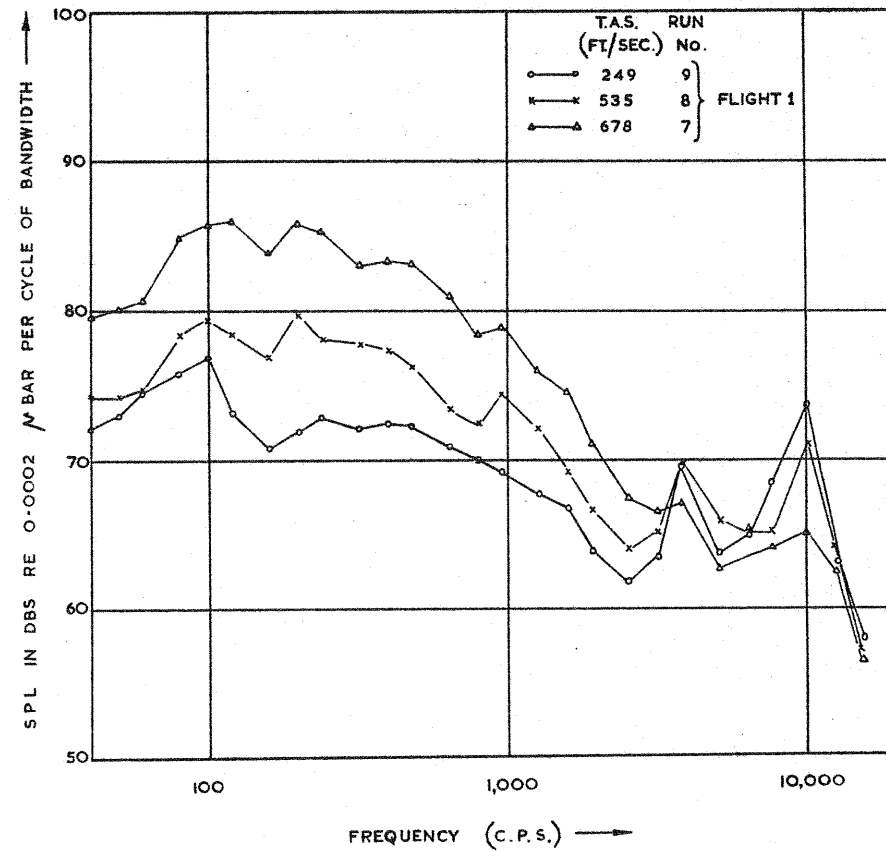


FIG. 7(b). SPECTRA (CORRECTED) - TRANSITION RING OFF.

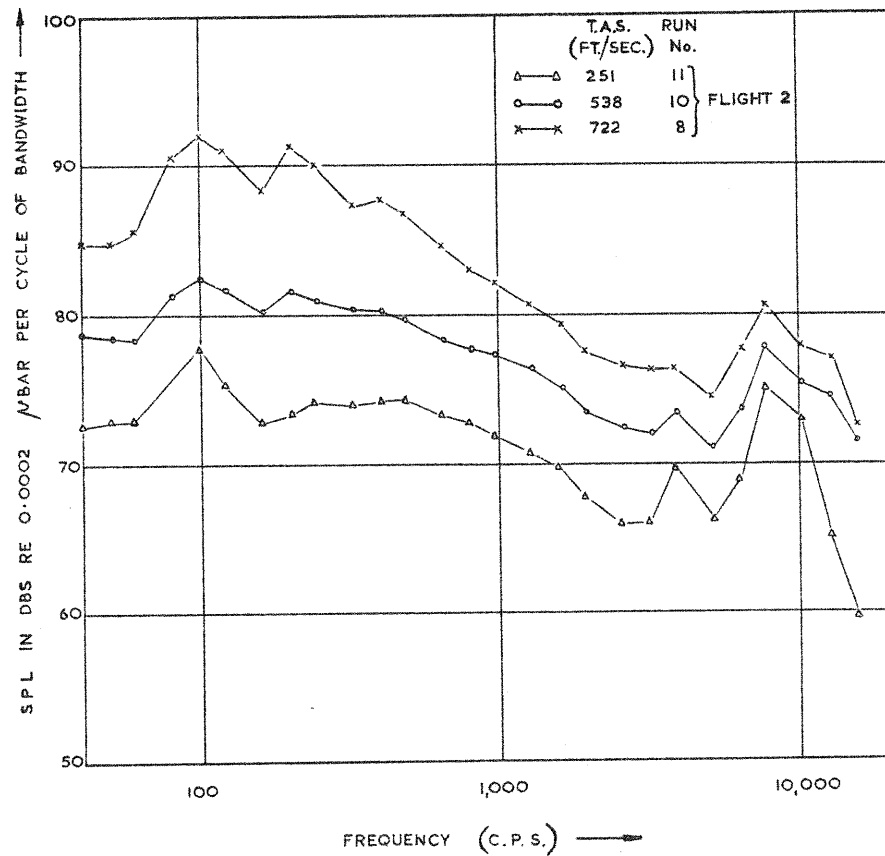


FIG 7(c) SPECTRA (CORRECTED) - TRANSITION RING ON.

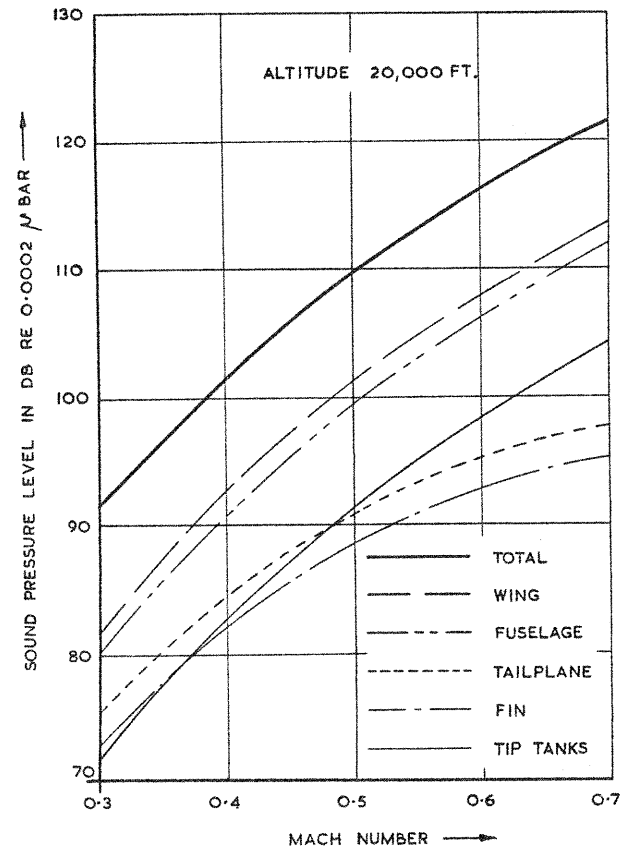
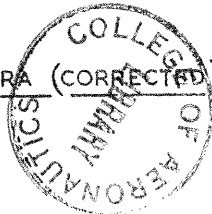


FIG. 8. CALCULATED OVERALL SPL AT MICROPHONE POSITION AS A FUNCTION OF MACH NUMBER.